Research on Chemical Intermediates
https://doi.org/10.1007/s11164-019-03737-z

Silica-coated $MgAl_2O_4$ nanoparticles supported phosphotungstic acid as an effective catalyst for synthesis of α-aminophosphonates

Reza Hajavazzade[1] · **Ali Reza Mahjoub**[2] · **M. Kargarrazi**[1]

Received: 10 November 2018 / Accepted: 2 January 2019
© Springer Nature B.V. 2019

Abstract

In this research, a recoverable catalyst ($MgAl_2O_4@SiO_2$–PTA) was prepared by a simple utilization method. The prepared catalyst was characterized by XRD, FT-IR, SEM, EDX, ICP-AES, and BET techniques. The average crystallite size of $MgAl_2O_4$ was calculated to be 40 nm by the Debye–Scherrer formula. The nanocomposite was examined as a heterogeneous catalyst for synthesis of α-aminophosphonates under solvent-free conditions at room temperature. In this process, magnesium aluminate spinel ($MgAl_2O_4$), used as the base and supporting catalyst for $H_3PW_{12}O_{40}$ (PTA), provides the recycling and reusing of the catalyst and also increases the efficiency of the reaction, which is due to the increase in the surface/volume ratio. In order to obtain optimal conditions, the synthesis of α-aminophosphonates reactions was investigated with different solvents and catalysts. The results showed that α-aminophosphonate prepared from the benzaldehyde and aniline reaction has higher efficiency and a shorter time than other reactions. The catalyst was recovered by simple filtration, and it can be recycled for at least five successive times without loss of catalytic activity.

Keywords Catalyst · Nanocomposite · α-Aminophosphonates · Heterogeneous catalyst · Solvent-free

---

Electronic supplementary material The online version of this article (https://doi.org/10.1007/s11164-019-03737-z) contains supplementary material, which is available to authorized users.

✉ Ali Reza Mahjoub
mahjouba@modares.ac.ir

[1] Department of Chemistry, Tehran North Branch, Islamic Azad University, Tehran, Iran

[2] Department of Chemistry, Faculty of Science, Tarbiat Modares University, P.O. Box 14155-4838, Tehran, Iran

Published online: 11 January 2019

Introduction

The choice of an effective modification on a catalyst can be improved by the selectivity, activity, and recycling properties. Recently, nanoparticles have attracted interest as solid supports for homogeneous catalysts immobilization [1, 2]. The nanoparticles can provide suitable media to access the substrate molecules due to the high surface-volume ratio. Meanwhile, it can be isolated efficiently from the product solution after completing the reactions [3, 4].

Polyoxometalates are a category of inorganic metal-oxide cluster group that can receive one or more electrons to yield species with mixed valence. Heteropolyacid (HPAs) catalysts have attracted considerable attention in industrial and academic fields due to their unique properties. Among various HPAs, hetropolyacid compounds of the Keggin structure have gained extensive applications, due to their strong activity, good catalytic properties, suitable redox sites, and selectivity for special reaction products [5–13]. Polyoxometalates have two major limitations: low surface area ($< 10\ m^2\ g^{-1}$) and solubility in polar solvents. These two interfere with the reaction efficiency and restrict the reusability of the catalysts. Most of the acidic protons are inaccessible for catalysts in nonpolar hydrocarbon reactions in bulk phosphotungestic acid. Supporting on nanoparticles is the main solution for improving the effective surface and solubility in polar solvents [14–17]. Mesoporous type materials such as silica, zeolites, alumina, zirconia, and, titania have been used as support for PTA [18–22]. Silica (SiO_2) is a typical mesoporous material and it has also attracted growing interest in diverse applications due to its chemical and physical stability, good biocompatibility and hydrophilic nature [23, 24]. The tedious recovery method via filtration and the indispensable loss of the solid catalyst in the separation process still limits its application, especially for the small nano-sized particles, while PTA supported on silica shows high catalytic efficiency and can be recycled more readily than its homogeneous counterpart method.

Magnesium aluminate ($MgAl_2O_4$) is one of the most important catalysts with much heat resistance and chemical and structural stability. It has various applications in humidity sensors, ceramic capacitors, fusion reactors, and catalysts [25, 26]. Magnesium aluminate has a low density (3.58 g/cm^3), high melting point (2135 °C), and good resistance against chemical attacks as well as very high temperatures [27]. Different methods for synthesis of spinel magnesium aluminate with particular characteristics, high purity, and low particle size have been reported, such as co-precipitation [28] of ions in solution, sol–gel [29, 30], microwave [31], solution combustion and solid state [32, 33]. Selecting the method depends on the chemical homogeneity of magnesium aluminate. These processes are mostly expensive or the environment limits them in large scale production. In general, smaller particle size with a higher surface area is suitable for various catalytic applications [34]. There were several types of research reported on silica-based composite materials and their applications [35–39].

In this study, a novel method is reported for immobilization of (PTA) silica coated magnesium aluminate nanoparticles. This nanocomposite was used as a catalyst for the preparation of α-aminophosphonates under solvent-free conditions at room temperature. In the recent few decades, α-aminophosphonates have been prepared using various methods and catalysts [40–42], (see Scheme 1).

Experimental

Materials and methods

All chemicals were purchased from Sigma-Aldrich or Merck with analytical grade and used as received. $H_3PW_{12}O_{40}$ (PTA) was purchased from Sigma-Aldrich. Fourier transform infrared (FT-IR) spectra were obtained using a FT BOMEM MB102 IR spectrophotometer. X-ray diffraction (XRD) patterns of the synthesized samples were recovered with a Philips X-ray diffractometer (model PW1730) The SEM and EDX images were obtained by a Hitachi Scanning Electron Microscope.

Synthesis of $MgAl_2O_4$@SiO_2–PTA nanocomposite

$MgAl_2O_4$ was prepared using the method reported by Mostafa Y. Nassar, with some minor modification [43]. To a coating of $MgAl_2O_4$ nanoparticles with a layer of silica, ethanol (1.5 ml), and, H_2O (10 ml) were mixed in a flask and were placed in an ultrasonic bath for 1 h. After that, NH_3 (1.5 ml) was added to this mixture. Then 2 g of $MgAl_2O_4$ particles were dispersed in it, and the mixture was vigorously stirred at 40 °C for 10 min. Then TEOS (0.53 ml) was added dropwise and mixing was continued for 1 h, and the mixture was stirred overnight. The coated particles were separated by filtration and washed with ethanol several times and dried at 80 °C in an oven. In this method for preparation of nanocomposite, ethanol/water (80:20 ratio) solution containing 1.0 g of PTA was mixed together, and the solution was stirred at room temperature for 1 h. Then, 1.0 g of $MgAl_2O_4$@SiO_2 was dispersed and stirred for an additional 3 h at the same temperature. The resulting solid was separated by filtration, and lastly, this nanocomposite was washed with absolute ethanol and dried in an oven at 100 °C for 2 h. The amount of PTA in $MgAl_2O_4$@SiO_2–PTA nanocomposite was determined by ICP-AES analysis to be 0.087 mmol g^{-1}. The typical preparation of composite ($MgAl_2O_4$@SiO_2–PTA) is shown in Scheme 2.

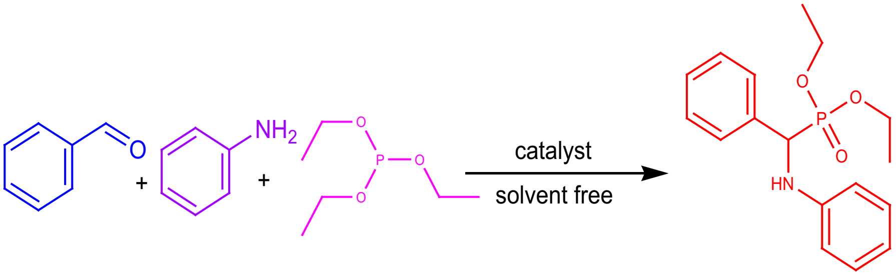

Scheme 1 $MgAl_2O_4$@SiO_2–PTA catalyzed synthesis of α-aminophosphonates

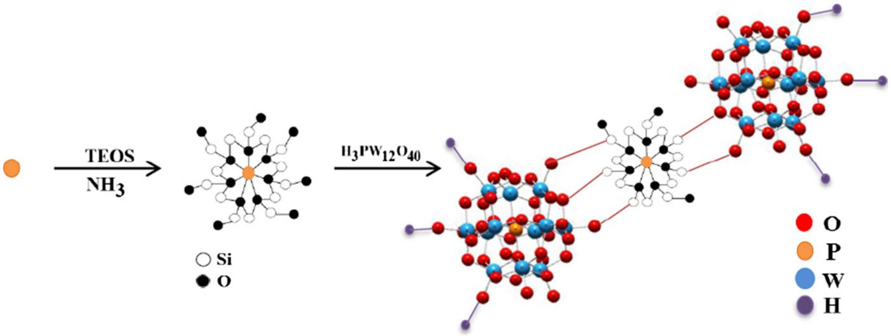

Scheme 2 Typical preparation procedure of the synthesis of $MgAl_2O_4@SiO_2$–PTA nanocomposite

General procedure of catalytic α-aminophosphonates synthesis

A mixture of aniline (1 mmol), aldehyde (1 mmol), triethyl phosphite (1.2 mmol) and $MgAl_2O_4@SiO_2$–PTA catalyst (0.05 g) was stirred at room temperature. The reaction was being monitored by TLC. Chloroform was added to dilute the reaction mixture, and the organic layer was simply isolated by filtration, at the end of the reaction. The isolated solution was purified on a silica-gel plate to obtain the pure product. The identities of the products were confirmed by FT-IR and ^{1}HNMR spectral data.

Results and discussion

Characterization of $MgAl_2O_4@SiO_2$–PTA composite

FT-IR spectra

$MgAl_2O_4@SiO_2$–PTA nanocomposite was manufactured via a simple procedure. $MgAl_2O_4$ was prepared by the sol–gel combustion method as a support for nanocomposite, then it was coated by a thin layer of silica. The synthesized nanocomposite was characterized by different techniques. The FT-IR spectra of all synthesized samples along with the pure PTA are presented in Fig. 1. In the IR spectra, the $MgAl_2O_4$ samples displayed two vibrations stretching at 555 cm^{-1} and 700 cm^{-1} consecrated to the $[AlO_6]$ groups, the lattice vibration of Mg–O stretching, and displaying the formation of $MgAl_2O_4$ spinel [44, 45]. Two vibrational bands at 3438 cm^{-1} and 1631 cm^{-1} appeared in the IR spectra of the products that could be attributed to the stretching and bending vibrations of the adsorbed surface molecular water interacting with $MgAl_2O_4$ [46–49]. Two bands were observed at 1063 cm^{-1} and 809 cm^{-1} which are ascribed to the symmetrical and asymmetrical vibrations of the Si–O–Si bonds. Two bands at 894 cm^{-1}

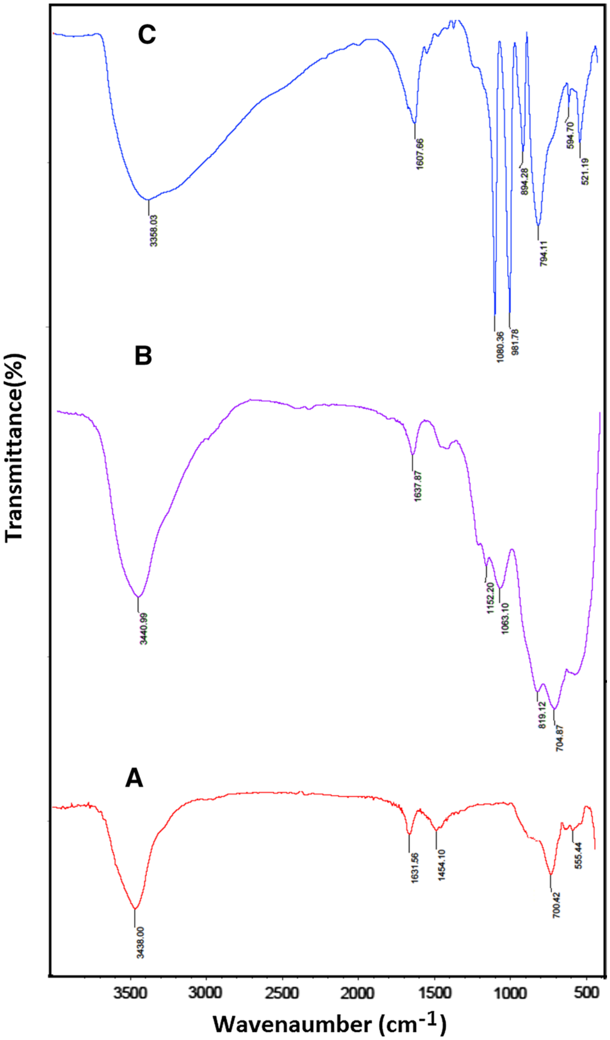

Fig. 1 FT-IR spectra of $MgAl_2O_4$ (**a**), $MgAl_2O_4@SiO_2$ (**b**) and $MgAl_2O_4@SiO_2$–PTA (**c**)

and 981 cm^{-1} are observed in the spectrum of $MgAl_2O_4@SiO_2$–PTA, which are respectively imputed to the W–O–W and W=O stretching modes of PTA [50, 51].

X-ray diffraction

The XRD patterns of $MgAl_2O_4$, $MgAl_2O_4@SiO_2$, $MgAl_2O_4@SiO_2$–PTA, are displayed in Fig. 2. The diffraction peaks related to Bragg's reflections from (111), (220), (311), (400), (422), (511), (440), and (533) planes corresponded to the standard spinel structure of $MgAl_2O_4$ (JCPDS Card No. 01-075-1798) (see Fig. 2a). The average crystallite size of $MgAl_2O_4$ nanoparticles was about 40 nm, as determined

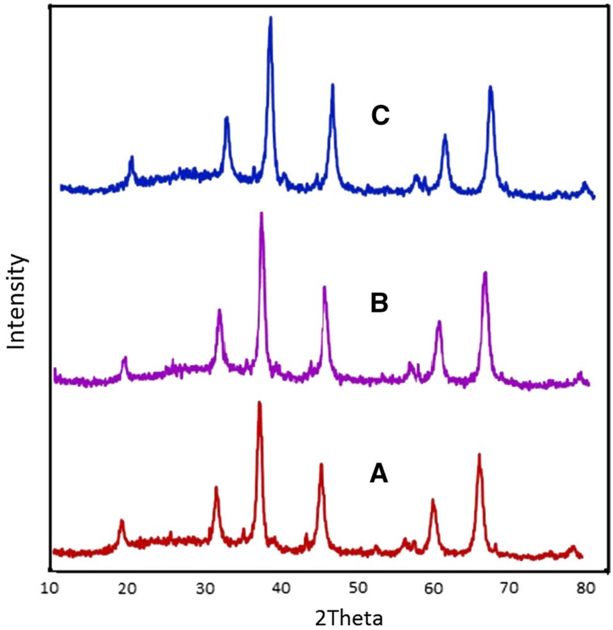

Fig. 2 XRD patterns of $MgAl_2O_4$ (**a**), $MgAl_2O_4@SiO_2$ (**b**), $MgAl_2O_4@SiO_2$–PTA(**c**)

using the Debye–Scherrer formula. The XRD patterns of $MgAl_2O_4$, after coating with silica and solitary with PTA are shown in Fig. 2b, c, which are more or less similar to the previous $MgAl_2O_4$ with the spinel structure.

Scanning electron microscopy (SEM)

The morphology of the samples was investigated by SEM. The SEM images of $MgAl_2O_4$, $MgAl_2O_4@SiO_2$ and $MgAl_2O_4@SiO_2$–PTA are presented in Fig. 3. SEM images display that $MgAl_2O_4$, $MgAl_2O_4@SiO_2$, and $MgAl_2O_4@SiO_2$–PTA particles are well dispersed and most of the prepared nanoparticles have spherical structure (Fig. 3a–c).

EDX microscopy and Brunauer–Emmett–Teller (BET) surface area analysis

The EDX spectrum is shown in Fig. 4. This spectrum obviously reveals the presence of all the expected main elements (O, Si, P, Al, Mg, and W) including the three mentioned component composites. The surface area of $MgAl_2O_4@SiO_2$–PTA was also estimated using the N_2 gas adsorption (BET) method and a value of 36.73 m^2 g^{-1}, average pore diameter is about: 15.00 nm and total pore volume: 0.1463 cm^3 g^{-1} were obtained for this composite. The graph of nitrogen adsorption–desorption isotherm of the $MgAl_2O_4@SiO_2$–PTA is presented in Fig. 5.

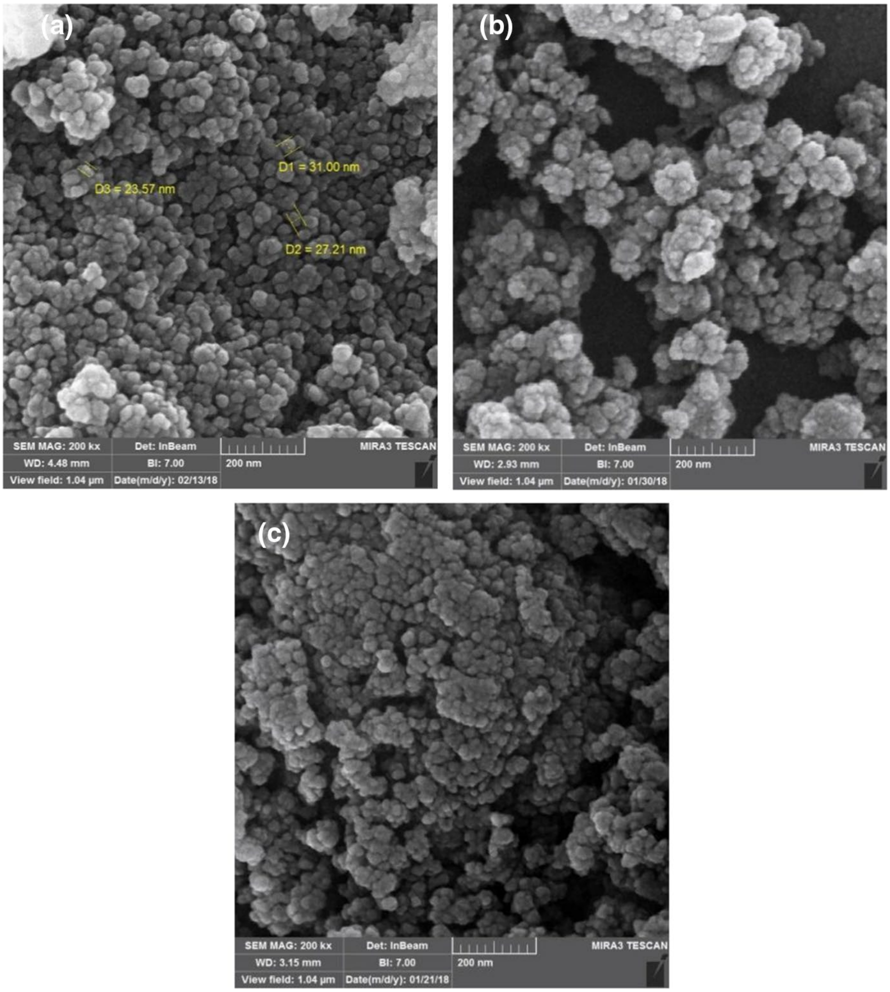

Fig. 3 SEM image of $MgAl_2O_4$ (**a**), $MgAl_2O_4@SiO_2$ (**b**), $MgAl_2O_4@SiO_2$–PTA(**c**)

α-Aminophosphonates synthesis

To optimize the reaction conditions of α-aminophosphonates synthesis, different portions were accomplished at room temperature by using aniline, benzaldehyde and triethyl phosphite as substrates in the presence of $MgAl_2O_4@SiO_2$–PTA as a catalyst. In order to obtain the best media, the various solvents such as H_2O, CH_3CN, C_2H_5OH, THF, DMF, Toluene, CH_2Cl_2, and solvent-free conditions were considered. The results are listed in Table 1. Much better results were received when this reaction was done with the solvent-free conditions (see Table 1).

$MgAl_2O_4$, $MgAl_2O_4@SiO_2$, $H_3PW_{12}O_{40}$, H_2SO_4, $SiO_2@Al_2O_3$, CuI, and in addition to $MgAl_2O_4@SiO_2$–PTA as catalysts studied, in order to obtain the effectiveness

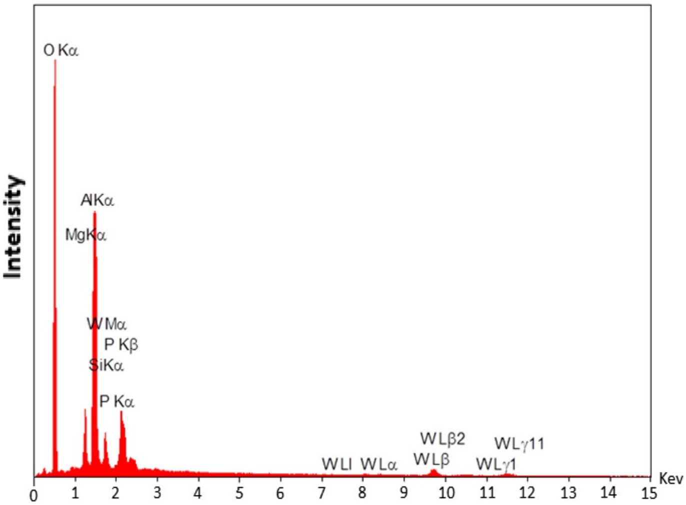

Fig. 4 EDX spectrum of $MgAl_2O_4@SiO_2$–PTA nanocomposite

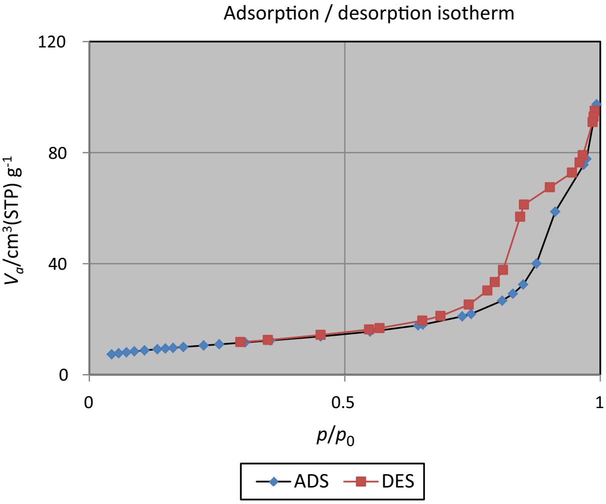

Fig. 5 Graph of nitrogen adsorption–desorption isotherm of the $MgAl_2O_4@SiO_2$–PTA

of PTA species on this catalytic reaction. As indicated in Table 2, $MgAl_2O_4@SiO_2$–PTA showed the best catalytic activity for the α-aminophosphates synthesis. The highest yield received was for aniline and benzaldehyde reaction.

The given results in Table 3 show that the condensations procedures were completed within 5–55 min, with good isolated yields with $MgAl_2O_4@SiO_2$–PTA used as a catalyst. The α-aminophosphonates syntheses have been reported in different methods [52–56]. These methods have been used under certain circumstances such as long reaction time, toxic catalysts, the presence of solvents and high temperature.

Table 1 Effect of various solvents on the synthesis of α-aminophosphonates

Entry	Solvent	Time	Yield (%)[a]
1	H_2O	50 min	80
2	CH_3CN	30 min	75
3	C_2H_5OH	45 min	72
4	Solvent free	5 min	97
5	THF	5 h	70
6	DMF	10 h	59
7	Toluene	8 h	75
8	CH_2Cl_2	30 min	82

All reaction conditions: benzaldehyde (1 mmol), aniline (1 mmol) $P(OEt)_3$ (1.2 mmol), catalyst (0.05 g) at room temperature

[a] Isolated yields

Table 2 Effect of various catalysts on the synthesis of α-aminophosphonates

Entry	Catalyst	Time (min)	Yield (%)[a]
1	$MgAl_2O_4$	120	–
2	$MgAl_2O_4@SiO_2$	120	–
3	$MgAl_2O_4@SiO_2$–PTA	5	97
4	$H_3PW_{12}O_{40}$	10	89
5	H_2SO_4	45	60
6	$SiO_2@Al_2O_3$	50	85
7	CuI	300	84

All reaction conditions: benzaldehyde (1 mmol), aniline (1 mmol), $P(OEt)_3$ (1.2 mmol), catalyst (0.05 g) at room temperature and solvent free

[a] Isolated yields

Since high yields of α-aminophosphates were obtained in solvent-free conditions and in a short reaction time at room temperature, these catalyst synthesis of α-aminophosphates can significantly reduce drawbacks. On the other hand, this catalyst can be separated from the reaction product by filtration and is recyclable several times with no noticeable loss in its activity.

Spectra data

Diethyl phenyl (phenyl amino) methyl phosphonate (Table 3, product of Entry 1) ^{1}HNMR (500MHZ, $CDCl_3$): δ 1.12–1.15 (t, 3H, CH_3), 1.29–1.32 (t, 3H, CH_3), 3.63–3.71 (m, 1H, CH_2), 3.90–3.97 (m, 1H, CH_2), 4.05–4.17 (m, 2H, CH_2), 4.74 (S, 1H), 4.79 (S, 1H), 6.58–6.60 (d, J = 10HZ, 3H), 6.68 (S, 1H), 6.69–6.71 (d, J = 10HZ, 1H), 7.09 (S, 1H), 7.10–7.12 (d, J = 10HZ, 2H), 7.25 (S, 1H), 7.28 (S, 1H), 7.32 (S, 1H), 7.33–7.35 (d, J = 10HZ, 2H), 7.46–7.48 (d, J = 10HZ, 3H). IR

Table 3 Synthesis of diversified α-aminophosphonates in the presence of $MgAl_2O_4@SiO_2$–PTA

Entry	Benzaldehyde	Amine	Time (min)	Yields (%)[b]
1	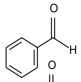	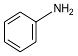	5	97
2	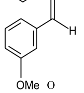	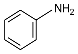	40	88
3	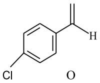	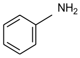	50	70
4	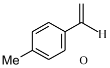	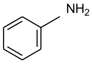	40	93
5	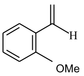	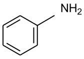	35	95
6	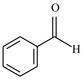	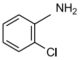	50	90
7	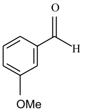	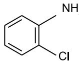	55	75
8	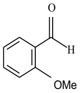	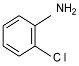	55	79
9	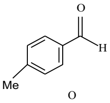	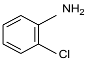	55	84
10	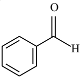	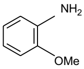	20	95
11	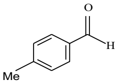	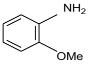	20	95
12	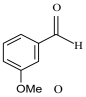	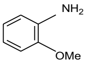	40	83
13	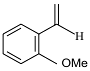	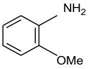	35	95
14 [a]	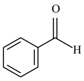	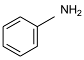	120	-

[a] Benzaldehyde (1 mmol), aniline (1 mmol), $P(OEt)_3$ (1.2 mmol), without catalyst at room temperature. All reaction condition: aldehydes (1 mmol), amine (1 mmol), $P(OEt)_3$ (1.2 mmol) and (0.05 g) of $MgAl_2O_4@SiO_2$–PTA at room temperature

[b] Isolated yields

(KBr) υ_{max}/cm^{-1}: 3294, 3048, 3029, 2982, 2934, 2908, 1605, 1525, 1497, 1454, 1391, 1365, 1273, 1236, 1058, 1017, 953, 798, 751, 734, 694, 572, 557.

Diethyl phenyl (phenyl amino) (m-tolyl) methyl phosphonate (Table 3, product of Entry 2) ^{1}HNMR (500 MHZ, $CDCl_3$): δ 1.12–1.14 (t, 3H, CH_3), 1.27–1.30 (t, 3H, CH_3), 3.66–3.74 (m, 1H, CH_2), 3.78 (S, 3H), 3.91–3.99 (m, 1H, CH_2), 4.05–4.17 (m, 2H, CH_2), 4.70 (S, 1H), 4.75 (S, 1H), 6.58–6.60 (d, J = 10 HZ, 2H), 6.68–6.70 (t, J = 10 HZ, 1H), 6.79–6.81 (d, J = 10 HZ, 1H), 7.01 (S, 1H), 7.05 (S, 1H), 7.06 (S, 1H), 7.08–7.12 (t, J = 10 HZ, 2H), 7.22–7.25 (t, 1H). IR (KBr) υ_{max}/cm^{-1}: 3301, 3033, 2979, 2904, 1601, 1530, 1497, 1466, 1439, 1387, 1365, 1250, 1030, 972, 869, 787, 745, 694, 600, 572.

Diethyl phenyl (phenyl amino) (O-ethyl) methyl phosphonate (Table 3, product of Entry 5) ^{1}HNMR (500 MHZ, $CDCl_3$): δ 1.04–1.07 (t, 3H, CH_3), 1.32–1.34 (t, 3H, CH_3), 3.59–3.67 (m, 1H, CH_2), 3.88–3.94 (m, 1H, CH_2), 3.69 (S, 3H), 4.16–4.23 (m, 1H, CH_2), 5.39 (S, 1H), 5.44 (S, 1H), 6.62–6.64 (d, J = 10 HZ, 2H), 6.67–6.70 (t, J = 10HZ, 1H), 6.90–6.94 (t, J = 10 HZ, 1H), 6.95 (S, 1H), 7.10 (S, 1H), 7.11–7.13 (d, J = 10 HZ, 1H), 7.23–7.25 (d, J = 10 HZ, 1H), 7.26 (S, 1H), 7.47–7.49 (d, J = 10 HZ, 1H). IR (KBr) υ_{max}/cm^{-1}: 3295, 3105, 3033, 2982, 2908, 2873, 1604, 1518, 1497, 1460, 1439, 1391, 1366, 1316, 1279, 1246, 1229, 1091, 1056, 1023, 969, 886, 796, 773, 747, 693, 583, 510.

Diethyl (2-methoxy phenyl amino) (P-tolyl) methyl phosphonate (Table 3, product of Entry 11) ^{1}HNMR (500 MHZ, $CDCl_3$): δ 0.88–0.94 (m, 1H), 1.14–1.17 (t, 3H, CH_3), 1.25–1.28 (t, 3H, CH_3), 2.3 (S, 3H), 3.69–3.80 (m, 1H, CH_2), 3.87 (S,3H), 3.94–4.04 (m, 1H, CH_2), 4.048–4.14 (m, 2H, CH_2), 4.70 (S, 1H), 4.75 (S, 1H), 6.40 (d, 1H), 6.42 (d, 1H), 6.62 (t, 1H), 6.65 (t, 1H), 6.68 (t, J = 10 HZ, 1H), 6.71 (t, J = 10 HZ, 1H), 6.74 (d, 1H), 6.76 (d, 1H), 7.11 (S, 1H), 7.12 (S, 1H), 7.26 (S, 3H), 7.33 (d, J = 10 HZ, 1H), 7.35 (d, 1H). IR (KBr) υ_{max}/cm^{-1}: 3422, 2982, 2932, 2835, 1601, 1511, 1456, 1431, 1391, 1367, 1244, 1050, 1023, 967, 833, 783, 740.

Recycling of the catalyst

The reusability of the catalysts is a major priority and has to be performed in heterogeneous methods. Recycling the $MgAl_2O_4@SiO_2$–PTA catalyst in this process can be performed in the same method as the tested one under the optimized conditions. The catalyst was gathered by filtering, followed by washing it twice with ethanol. Then it was dried at 100 °C for 2 h, after that, it was reused in a new reaction. The results are presented in Table 4. The recovered catalyst could be reused for five successive times without any changes in the activity (see Table 4). The FT-IR spectrum of the recovered catalyst showed no changes after it has been used for five successive times (see Fig. 6).

Table 4 Reusability of $MgAl_2O_4@SiO_2$–PTA catalyst in the model reaction

Entry	Time (min)	Yield (%)[a]
Fresh	5	97
1	5	96
2	5	94
3	5	93
4	5	92
5	5	91

All reaction conditions: benzaldehyde (1 mmol), aniline (1 mmol), $P(OEt)_3$ (1.2 mmol), $MgAl_2O_4@SiO_2$–PTA as catalyst (0.05 g) at room temperature and solvent free

[a] Isolated yields

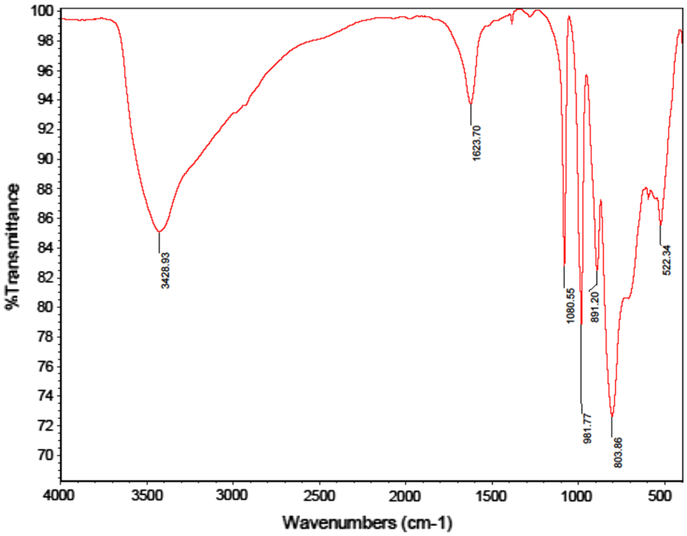

Fig. 6 FT-IR spectra of catalyst: recycled catalyst after five runs

Proposed mechanism for synthesis of α-aminophosphonates

Scheme 3 represents the proposed mechanism for the preparation of α-aminophosphonates. This reaction is likely to be accelerated by the phosphonate activated imine. As indicated in the Scheme 3, in this reaction, the phosphonium intermediate is formed by the nucleophilic addition of triethyl phosphite to the imine, then it reacts with the water produced from the imine formation phase, and forms α-aminophosphonate and ethanol [57] (see Scheme 3).

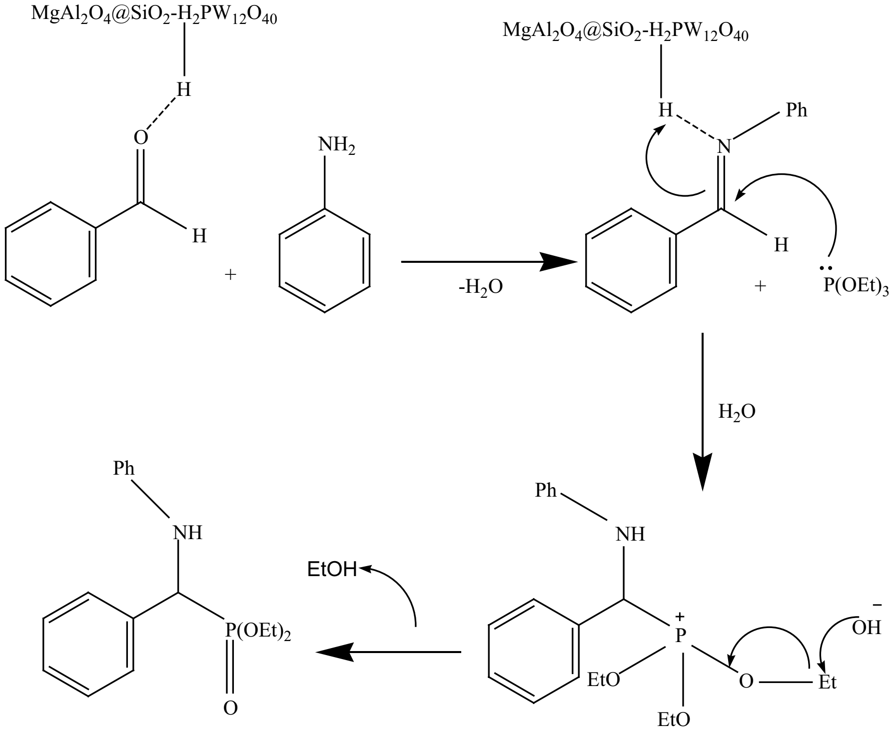

Scheme 3 Proposed mechanism for synthesis of α-aminophosphonates

Conclusions

In this research, fabrication of a novel nanocomposite as a catalyst using $MgAl_2O_4$ nanoparticles as support via a simple procedure was studied. The synthesized catalyst was considered by XRD, FT-IR, SEM, EDX, ICP-AES, and BET techniques. This catalyst was used in some α-aminophosphates reactions under solvent-free conditions, at room temperature in short reaction times. This nanocomposite reaction was carried out under solvent free conditions, that can be considered as a "green procedure". The immobilized PTA catalyst could be recovered by simple filtration and reused at least five times without significant loss of activity.

Acknowledgements Financial support of this paper by Tehran North Branch, Islamic Azad University, and Tarbiat Modares University, is thankfully acknowledged. Also acknowledged is Reza Hajavazzade, Ph.D. student who did all the experiments, Alireza Mahjoub, Supervisor of the project, and Maryam Kargar Razi, Advisor of the project.

References

1. C.W. Lim, I.S. Lee, Nano Today **5**, 412 (2010)
2. S. Shylesh, V. Schunemann, W.R. Thiel, Angew. Chem. Int. Ed. **49**, 3428 (2010)

3. R. Abu-Rezig, H. Alper, D. Wang, M.L. Post, J. Am. Chem. Soc. **128**, 5279 (2006)
4. P. Riente, C. Mendoza, M.A. Pericas, J. Mater. Chem. **21**, 7350 (2011)
5. N.Y. He, C.S. Woo, H.G. Kim, H.I. Lee, Appl. Catal. A **281**, 167 (2005)
6. G.S. Kumar, M. Vishnuvarthan, M. Palanichamy, V. Murugesan, J. Mol. Catal. A: Chem. **260**, 49 (2006)
7. I.V. Kozhevnikov, J. Mol. Catal. A: Chem. **262**, 86 (2007)
8. A. Kumar, P. Singh, S. Kumar, R. Chandra, S. Mozumdar, J. Mol. Catal. A: Chem. **276**, 95 (2007)
9. M.H. Bhure, I. Kumar, A.D. Natu, R.C. Chikate, C.V. Rode, Catal. Commun. **9**, 1863 (2008)
10. R.T. Carr, M. Neurock, E. Iglesia, J. Catal. **278**, 78 (2011)
11. A. Ciftci, D. Varisli, C.K. Tokay, N.A. Sezgi, T. Dogu, Chem. Eng. J. **207–208**, 85 (2012)
12. A.M.I. lnicka, E. Bielanska, L.L. Dobrzynska, A. Bielanski, Appl. Catal. A **421–422**, 91 (2012)
13. H. Haddadi, S. Moradpour Hafshejani, M. Riahi Farsani, A. Kazemi Babahydari, New J. Chem. **39**, 9879 (2015)
14. J. Kaur, K. Griffin, B. Harrison, J. Catal. **208**, 448 (2002)
15. T. Tagawa, J. Amemiya, S. Goto, Appl. Catal. A **257**, 19 (2004)
16. H. Kim, J.C. Jung, S.H. Yeom, K.Y. Lee, I.K. Song, J. Mol. Catal. A: Chem. **248**, 21 (2006)
17. Z. Obali, T. Dogu, Chem. Eng. J. **138**, 548 (2008)
18. Y. Kamiya, T. Okuhara, M. Misono, A. Miyaji, K. Tsuji, T. Nakajo, Catal. Surv. Asia **12**, 101 (2008)
19. X.M. Yan, P. Mei, J.H. Lei, Y.Z. Mia, L. Xiong, L.P. Guo, J. Mol. Catal. A: Chem. **304**, 52 (2009)
20. B.S. Li, W. Ma, J.J. Liu, C.Y. Han, S.L. Zuo, X.F. Li, Catal. Commun. **13**, 101 (2011)
21. G.S. Armatas, G. Bilis, M. Louloudi, J. Mater. Chem. **21**, 299 (2011)
22. R.M. Ladera, J.L.G. Fierro, M. Ojeda, S. Rojas, J. Catal. **312**, 195 (2014)
23. Y. Sun, L. Duan, Z. Guo, Y.D. Mu, M. Ma, L. Xu, Y. Zhang, N. Gu, J. Magn. Magn. Mater. **285**, 65 (2005)
24. Y. Wang, H. Katepalli, T. Gu, T.A. Hatton, Y. Wang, Langmuir **34**, 2674 (2018)
25. M.J. Iqbal, B. Ismail, C. Rentenberger, H. Ipser, Mater. Res. Bull. **46**, 2271 (2011)
26. E. Amini, M. Rezaei, B. Nematollahi, J. Porous Mater. **22**, 481 (2015)
27. B. Ismail, S.T. Hussain, S. Akram, Chem. Eng. J. **219**, 395 (2013)
28. H. Li, Y.Q. Liu, Z.J. Yang, Mater. Res. Innov. **19**, 20 (2015)
29. S. Sanjabi, A. Obeydavi, J. Alloy. Comp. **645**, 535 (2015)
30. N. Habibi, Y. Wang, H. Arandiyan, M. Rezaei, Adv. Powder Technol. **28**, 1249 (2017)
31. H.B. Bafrooein, T. Ebadzadeh, Cera. Int. **39**, 8933 (2013)
32. R. Ianos, I. Lazau, C. Pacurariu, P. Barvinschi, Mater. Res. Bull. **43**, 3408 (2008)
33. N. Rahmat, Z. Yaakob, M. Pudukudy, N.A. Rahman, S.S. Jahaya, Powder Technol. **329**, 409 (2018)
34. P.V.M. Kutty, S. Dasgupta, Ceram. Int. **39**, 7891 (2013)
35. O. Olkhovyk, M. Jaroniec, J. Am. Chem. Soc. **127**, 60 (2005)
36. Z. Qiao, L. Zhang, M. Guo, Y. Liu, Q. Huo, Chem. Mater. **21**, 3823 (2009)
37. H. Chaudhuri, S. Dash, A. Sarkar, RSC Adv. **6**, 99444 (2016)
38. H. Chaudhuri, S. Dash, R. Gupta, D.D. Pathak, A. Sarkar, Chem. Sel. **2**, 1835 (2017)
39. H. Chaudhuri, R. Gupta, S. Dash, Catal. Lett. **148**, 1703 (2018)
40. X. Rao, Z. Song, L. He, Hetero Chem. **19**, 512 (2008)
41. I. Kraicheva, A. Bogomilova, I. Tsacheva, G. Momekov, K. Troev, Eur. J. Med. Chem. **44**, 33 (2009)
42. K. Ramakrishna, J. Mary Thomas, C. Sivasankar, J. Org. Chem. **81**, 9826 (2016)
43. M. Nassar, I. Ahmed, I. Samir, Spectra Chem Act. Part A. Mol. Biomol. Spect **131**, 329 (2014)
44. S.M. Olhero, I. Ganesh, P.M.C. Torres, J.M.F. Ferreira, Langmuir **24**, 9525 (2008)
45. J. Puriwat, W. Chaitree, K. Suriye, S. Dokjampa, P. Praserthdam, J. Panpranot, Catal. Commun. **12**, 80 (2010)
46. M.Y. Nassar, I.S. Ahmed, Polyhedron **30**, 2431 (2011)
47. M.Y. Nassar, I.S. Ahmed, Mater. Res. Bull. **47**, 2638 (2012)
48. M.Y. Nassar, A.S. Attia, K.A. Alfallous, M.F. El-Shahat, Inorg. Chem. Act. **405**, 362 (2013)
49. M.Y. Nassar, Mater. Lett. **94**, 112 (2013)
50. T. Rakjumar, G.R. Rao, J. Chem. Sci. **120**, 587 (2008)
51. R. Khoshnavazi, L. Bahrami, F. Havasi, E. Naseri, RSC. Adv. **7**, 11510 (2017)

52. M. Tajbakhsh, A. Heydari, H. Alinezhad, M. Ghanei, S. Khaksar, Synthesis **3**, 352 (2008)
53. M. Ordonez, H. Rojas-Cabrera, C. Cativiela, Tetrahedron **65**, 17 (2009)
54. Z. Rezaei, H. Firouzabadi, N. Iranpoor, A. Ghaderi, M.R. Jafari, A.A. Jafari, H.R. Zare, Eur. J. Med. Chem **44**, 4266 (2009)
55. Z. Yan, B. Wu, X. Gao, M. Wang Chen, Y. Gui Zhou, Org. Lett. **18**, 692 (2016)
56. M. Kollia, P. Elamathia, G. Chandrasekara, V. Rao Kattab, G. Balvantsinh Raoljib, Synth. Commun **48**, 638 (2018)
57. J. Akbari, A. Heydari, Tetra. Lett. **50**, 4236 (2009)

Publisher's Note Springer Nature remains neutral with regard to jurisdictional claims in published maps and institutional affiliations.